Heating Efficiencies with and without Impurities for Neutral Injection in the W VII A Stellarator

S. Rehker

IPP 2/237 February 1978

MAX-PLANCK-INSTITUT FÜR PLASMAPHYSIK

8046 GARCHING BEI MÜNCHEN

MAX-PLANCK-INSTITUT FÜR PLASMAPHYSIK

GARCHING BEI MÜNCHEN

Heating Efficiencies with and without Impurities for Neutral Injection in the W VII A Stellarator

S. Rehker

IPP 2/237 February 1978

Die nachstehende Arbeit wurde im Rahmen des Vertrages zwischen dem Max-Planck-Institut für Plasmaphysik und der Europäischen Atomgemeinschaft über die Zusammenarbeit auf dem Gebiete der Plasmaphysik durchgeführt.

IPP 2/237 S.Rehker

Heating Efficiencies with and without Impurities for Neutral Injection in the W VII A Stellarator.

February 1978

Abstract

This paper investigates the influence of the magnetic field configuration of a stellarator (W VII A) on the properties of a neutral injection experiment. Impurity effects, such as beam shielding and sputtering, are estimated. Assuming a particle confinement time for sputtered particles, radiation losses of these particles are calculated. Reduced heating efficiencies for neutral injection are given with allowance for these losses.

I. Introduction

The heating efficiency of a neutral injection experiment depends on the impurities which are already present in the plasma or which are introduced by neutral injection. Of all possible problems associated with impurities in a neutral injection experiment two major questions are investigated in this paper. Firstly, a high impurity content within the target plasma for neutral injection could drastically change the absorption profile. A high impurity concentration could even shield the plasma from the fast injected particles, as has been pointed out in Ref. 1) 2).

The second problem associated with impurities is the enhanced sputtering at the wall or the limiter (stainless steel and other materials). This is because fast injected particles might be scattered into (or even born on) nonconfined orbits. By increasing the impurity content in the plasma this problem is in turn coupled to the first one.

Both of these problems are well known and have been partly investigated in the past [3], but the calculations here were made for a tokamak geometry only. The validity of these calculations for stellarator configurations, such as the W VII A, is limited because the drift orbits of fast particles are drastically changed compared with those in a tokamak configuration. A proper estimation of the heating efficiency and the impurity problems mentioned above has to take the full three-dimensional character of the stellarator field into account. Calculations of the three-dimensional problems in tokamak configurations (main field ripple) were made - at least in the Monte-Carlo sense - by Mary and Dei-Cas using the modified Gourdon magnetic field program [4]. With the kind help of Dr. Dei-Cas this code has been implemented at IPP and modified by the author to take the W VII A stellarator geometry into account.

In order to clarify the effects introduced by the stellarator windings in the W VII A neutral injection experiment, the stellarator configuration is compared with a hybrid configuration - stellarator with plasma current - and with a tokamak, the geometrical configurations beeing the same.

The problems connected with beam trapping by impurities are investigated in Section 3 and sputtering from the stainless steel wall is investigated in Section 4. The radiation losses by the sputtered Fe-ions are estimated there on the basis of figures given by Breton et al.[6] and give rise to effective heating efficiencies for neutral injection.

II. Heating efficiencies

After ionization the fast particles will undergo Coulomb scattering in the plasma during thermalization. Some of the fast particles will be scattered to the loss cone, thus reducing the energy given to the plasma and increasing the sputtering rates. The fraction of energy given to the plasma relative to the energy in the neutral beam is called the heating efficiency W. The values calculated by the simulation code are given below although some of the figures have already been given by W. Ott and E. Speth[5].

The W VII A stellarator has a major radius of $R_m = 200$ cm and a limiter radius of $r_L = 13$ cm. The $l = 2$, $m = 5$ stellarator field, which is described in detail in Ref. 14, is produced by conventional helical windings. The stellarator field deforms the plasma column elliptically. To allow for this deformation, the plasma radius chosen in the numerical simulation experiment is $a = 10$ cm. For comparison, the same value is chosen in the tokamak case, although this will be an underestimation of the heating efficiency in this case.

The plasma profiles which govern the beam capture and the heating efficiency properties are assumed to be the following:

We assume the plasma current density to be of the form

$$j(r) = j(0)\ (1 - (\tfrac{r}{a})^2)^q \quad \text{for} \quad r \leqslant a,$$

which is consistent with present measured data.

Here we take $a = 10$ cm; $q \simeq 2.7$ and

$$I_\varphi = \frac{j(0)\,\pi\,a^2}{q+1} = 32 \text{ kA}.$$

The electron temperature profile is assumed to be

$$T_e(r) = T_{e,max}\,(1 - (\frac{r}{a})^2)^{4/3} \quad \text{for } r \leqslant a = 10 \text{ cm}.$$

The calculations were done for two values of $T_{e,\,max}$,

$$T_{e,\,max} = 0.3 \text{ keV} \quad \text{and} \quad T_{e,max} = 1 \text{ keV}.$$

The electron density profile was taken as

$$n_e(r) = 2 \cdot 10^{14}\,(1 - (\frac{r}{a})^2)^2 \quad \text{for } r \leqslant a = 10 \text{ cm}.$$

It should be emphasized at this point that the heating efficiencies W will decrease drastically in all configuration types if this high plasma density cannot be achieved for the target plasma for neutral injection. At present the maximum electron density reached in W VII A is $n_{e,max} = 8 \times 10^{13}\,\text{cm}^{-3}$ (hybrid case).

In the following we compare three magnetic field configurations which can be realized in the W VII A experiment.

a) W VII A stellarator with helical windings which produce a rotational transform of $\iota_H = 0.23$. Here the ohmic plasma current is set to 0 . ("pure stellarator")

b) W VII A stellarator with helical windings as above but with ohmic heating current of 32 kA. ("hybrid case")

c) W VII A geometry with ohmic heating current of 32 kA without helical currents. ("tokamak case")

Having defined the magnetic configuration and the geometry as above, the injection experiment is simulated by the code in the following way[+] :

[+] This is a simplified description. For further information see Ref. 4) .

First the intersection points of the injection line with the plasma torus are calculated. The interval between these points is divided in up to 50 sections. Each of these sections is assigned one particle which carries a weight corresponding to the fraction of fast particles captured from the beam within this section. The total capture cross-section can be written as follows:

$$\sigma_c = \sigma_{cx} \frac{n_i}{n_e} + \frac{\langle \sigma_{ie} v_e \rangle}{v} + Z_{eff} \sigma_{pi} .$$

The first term is due to charge exchange processes with plasma ions, the second term to ionization by electrons, and the third term to ionization by protons. Here the ionization collisions with impurities were taken into account with the factor Z_{eff} in the original code. The initial conditions of the simulation particles, viz the start point and velocity components, are therefore known. The guiding centre equations of the particles are thus integrated in the given field together with an equation for the energy which describes the slowing down. These equations are given in detail in Ref.4. Using a pseudo-random number generator, collisions between the fast particles and the plasma are introduced. The angle of the scattering cone is chosen to be consistent with the Spitzer formula

$$\tau_{sc} = \frac{\langle (\Delta v_\perp)^2 \rangle}{v^2} ,$$

which is the scattering time for 90° deflection. These collisions change the direction of velocity of the simulation particles and can thus lead to non-confined orbits. The "history" of all particles is recorded, so that the energy deposition profile and other data can be evaluated at the end of each simulation run.
The error introduced by the Monte-Carlo procedure can be estimated and kept small by repeating the calculation. In most cases the values given for the heating efficiency are calculated with a standard error of the mean, ΔW, smaller than 3%.

With the maximum injection angle of 5.5^{o} which is possible for the W VII experiment we calculate the following heating efficiencies:

For $E_{beam} = 10$ keV and $T_{e,max} = 0.3$ keV we obtain

a) pure stellarator: $W = (40 \pm 3.5)$ %

b) hybrid case: $W = (67 \pm 2)$ %

c) tokamak case: $W = (79 \pm 2)$ %

The predominant part of the beam consists of 10 keV particles ($I_{eq} = 139$ A), but there are other parts with energies of 15 keV ($I_{eq} = 16$ A) and 30 keV ($I_{eq} = 8$ A). The heating efficiencies calculated for $E_{beam} = 15$ keV were:

a) pure stellarator: $W = (29 \pm 2)$ %

b) hybrid case: $W = (45 \pm 3)$ %

c) tokamak case: $W = (77 \pm 3)$ %

and for $E_b = 30$ keV:

a) pure stellarator: $W = (6 \pm 1)$ %

b) hybrid case: $W = (25 \pm 2)$ %

c) tokamak case: $W = (62 \pm 1)$ %

For all injection energies the heating efficiencies are rather low in the stellarator case. The ohmic heating current improves the properties of the stellarator configuration. It should be emphasized that the poor heating efficiency for the 30 keV part of the beam would make the neutral injection impossible in the stellarator case, whereas the values are still reasonable for the tokamak.

In the estimates relating to impurities in the following sections only the 10 keV part of the beam will be considered. But it should be kept in mind that the high-energy fraction of the beam has lower heating efficiencies, especially for the stellarator case; thus the results presented below for the sputtering estimates are optimistic in this case.

The reason for the big differences between stellarator and tokamak is illustrated in the figures. In Fig.1 the particle coordinates during the thermalization are projected onto a meridional plane. Collisions are marked by crosses. Three examples

are given for each configuration. The spiralling paths described by the particles in the stellarator field allow collisions near the plasma boundary. However, collisions near the plasma boundary will lead to losses with a high probability. In the tokamak case we get the common banana trajectories which are comparatively regular and localized.

In the next figures (2 - 4) the captured fraction of the beam along the injection path in the plasma is plotted. The heating efficiencies in each of the 50 sections are calculated. The energy given to the plasma from particles born in the specified section is the product of the captured fraction and the heating efficiency. This value is denoted by the lower extremities of the histogram in Figs.2 - 4. The jumps are due to statistical fluctuations. The difference between the lower and upper extremeties (shaded area) is proportional to the energy loss due to collisions. As may be seen from the plot in the tokamak case (Fig.4), particle losses from the plasma centre are rare, whereas in the stellarator case (Fig.2) an appreciable amount of energy is transported to the wall even from the plasma centre.

If the plasma temperature is increased by neutral injection from $T_{e,max} = 0.3$ keV to $T_{e,max} = 1$ keV, the slowing-down time increases. The heating efficiencies for $E_{beam} = 10$ keV are calculated in this case to be

a) pure stellarator: $W = (13 \pm 2)$ %
b) hybrid case: $W = (37 \pm 6)$ %
c) tokamak case: $W = (47 \pm 3)$ %

The tokamak case still gives the best heating efficiency.

III. Impurity trapping

As pointed out by Girard, Marty and Moriette[1], an impurity beam trapping instability could occur during neutral injection. For a stellarator configuration this effect would be especially dangerous because particles which are born near the plasma boundary have a higher chance of getting lost than in a tokamak.

The simulation code[4] has therefore been modified to account for up to 10 species of impurities $n_{z,j}$. The charge and the charge exchange cross-section $\sigma_{cx,j}$ with the beam particles can be individually prescribed. The profiles for Z_{eff} and n_i are then calculated from

$$n_e = n_i + \sum_{j=1}^{10} Z_j^2 \, n_{z,j} \,,$$

$$Z_{eff} = \frac{1}{n_e} \left(n_i + \sum_{j=1}^{10} Z_j^2 \, n_{z,j} \right) .$$

The total beam capture cross-section is extended to

$$\sigma_c = \sigma_{cx} \frac{n_i}{n_e} + \frac{\langle \sigma_{ie} \, v_e \rangle}{v} + Z_{eff} \sigma_{pi} + \frac{1}{n_e} \sum_{j=1}^{10} n_{z,j} \, \sigma_{cx,j} \,.$$

Here the first three terms are explained in the preceeding section. The last term now includes the charge-exchange collisions of beam particles with impurities.

Of interest in the W VII A stellarator is the influence of charge exchange collisions of the beam particles with oxygen impurities which will be present in the target plasma on the beam capture profile. The density of oxygen impurities in the plasma can be estimated on the basis of today's spectroscopic measurements[7]. However, the neutral injection will also increase the impurity level by sputtering at the wall. The influence of these heavy impurities on the beam capture profile is additionally estimated on the basis of the calculations given in the following section.

To calculate the beam capture profile, the charge exchange cross-sections $\sigma_{cx,i}$ must be known. Fortunately, since the first calculations by Moriette[8] new calculations have been made by Olson and Salop[9)10)] and others. The values given by these authors are smaller than those given by Moriette. Recently, the available data were compiled by the TFR team[11)]. The values for the charge exchange cross-sections used here were taken from this paper. The charge exchange cross-section for highly ionized Fe-ions was estimated to be $\sigma_{cx,Fe} = 1.5 \cdot 10^{-14}\ cm^2$. The results of the computations are given in Fig.5. In this figure the beam capture profile along the injection path is plotted for three cases:

a) beam capture without impurities
b) beam capture with oxygen impurities (approx. 1%)
c) beam capture with oxygen impurities and Fe impurities (approx. .1%) due to sputtering.

As can be seen from this figure, the influence of the impurities which can be expected in the W VII A plasma on the beam capture profile and hence on the heating efficiency is small. This effect therefore does not seem to be important in the W VII A experiment.

IV. Sputtering

Estimations of the sputtering rate which can be expected on W VII A owing to neutral injection have been made by Ott, Speth and Staebler[12)] for the tokamak case. However, as has been shown in Sec.II, the number of particles which hit the wall increases drastically in the stellarator case. The Monte-Carlo code used here affords the possibility of estimating the effects of sputtering more realistically than in Ref.12. The procedure used is briefly described in the following:

The injected beam with intensity I_E either is absorbed (I_A) or will not be captured (I_{NC}):

$$I_E = I_A + I_{NC} \quad .$$

As has been described above, the absorbed fraction is simulated by the code by up to 50 particles. Each of these particles carries a weight corresponding to the captured fraction of the specific section on the injection line. This weight is denoted by W_c (j). The intensity balance equation can therefore be written

$$I_E = I_E \quad \left(\sum_{j=1}^{50} W_c(j) + W_{NC} \right).$$

If the integration of the particle trajectory and the Monte-Carlo procedure show that the simulation particle is scattered into an unconfined orbit, the simulation particle will cause sputtering at the wall. For these particles the code calculates both impact intensity and energy. Taking the sputtering coefficient S (E) given by Scherzer[13], the flux of sputtered Fe-atoms from the wall is then calculated. The accuracy of this flux is given by the Monte-Carlo procedure. As was the case for the heating efficiency, the statistical error can be made small by repeating the calculation.

To estimate the Fe-impurity density we assume that all sputtered Fe-atoms will reach the plasma and will be ionized within the plasma. In the worst case all sputtered Fe-ions will accumulate in the plasma centre. However, we assume the more optimistic case that the particle confinement time τ_p measured for the plasma in today's experiments will be valid for the Fe-ions, too. An equilibrium will therefore be reached within one particle confinement time after the start of neutral injection. We further assume the Fe-impurity density to be constant in space. With the data given by Breton et al.[6] we can then estimate the radiated power from the Fe-impurities and calculate a reduced effective heating efficiency W' which takes the radiation into account:

$$W' = \frac{\text{injected power} * \text{heating efficiency (W)} - \text{total radiated power } (P_{tot})}{\text{injected power}}$$

The results of the calculations which were made only for the 10 keV part of the beam are summarized in Table I. The other parts of the beam (15 keV and 30 keV) would increase the sputtering rates especially for the stellarator case, so that

the figures given in Table I are optimistic in this case. The absolute values given there are obtained for a beam intensity of $I_{B,eq} = 139$ A for the 10 keV part of the beam and for a particle confinement time of $\tau_p = 20$ ms. A higher particle confinement time will increase the impurity level and hence the radiation losses. The influence of such impurity levels on the beam trapping has been shown in the preceeding section to be unimportant (Fig. 5).

V. Conclusions

This paper investigates the influence of the magnetic field configuration of a stellarator on the properties of a neutral injection experiment. The stellarator configuration (W VII A) is compared with a tokamak and with a hybrid configuration of equal geometrical size. It is found that the heating efficiency for the stellarator is only reasonable for beam energies smaller than 10 keV, whereas the heating efficiency is still good in a tokamak for beam energies of 30 keV.

For comparison purposes the calculations were done with an equal effective plasma radius. However, the real plasma radius would be larger in the tokamak so that the numbers given here are even pessimistic for the tokamak case.

The sputtering rates on the stainless steel vacuum vessel were calculated by analyzing the particle and energy losses. On the basis of a particle confinement time for the sputtered impurities the radiation loss due to these impurities was estimated. This loss reduces the heating efficiency from $W \approx 40\%$ to $W' \approx 20\%$ in the stellarator case.

The influence of the sputtered impurities in addition to the impurities which might already be in the plasma on the beam capture profile was investigated. It turned out, however, that the beam capture profile will not be appreciably changed by the presence of these impurities.

The calculations given here were made for the most promising injection angle which seems experimentally possible. A higher injection angle would increase the heating efficiencies but the tokamak configuration would still be an upper limit.

References

1) J.P.Girard, D.H.Marty and P.Moriette, Proc. 5th Conf. on Plasma Physics and Controlled Nuclear Fusion (1975) p.681

2) J.T.Hogan and H.C.Howe, An Impurity Beam Trapping Instability in Tokamaks, ORNL/TM-5361 (1976)

3) J.H.Feist, W.Ott, E.Speth, Proc. of the Int.Symp.on Plasma Wall Interaction (1976) p.69

4) Dei-Cas, private communication

5) W.Ott and E.Speth, Neutral Injection into W VII A Stellerator - Calculation of Ion Trajectories and Heating Efficiencies, lecture given on Stellarator Symposium , CSSR (1977)

6) C.Breton, C.Michelis, M.Mattioli, EUR-CEA-FC 853 (1976)

7) H.Hacker, W VII A team, private communication

8) P.Moriette, Ionization and Charge Exchange Cross Sections in Collisions between heavy Multicharged Ions and Neutral Atoms. Proc. 7th Jugosl. Symp.on the Physics of Ionized Gases, Contr.Papers p.43 (1974)

9) R.E.Olson and A.Salop, Phys. Rev. A 14, 579 (1976)

10) R.E.Olson and A.Salop, Phys.Rev. A 16, 531 (1977)

11) TFR-Team, Neutral Beam Attenuation Measurements in TFR. Determination of Ion Density and Z_{eff}. Report under preparation.

12) W.Ott, E.Speth, H.Stäbler, IPP 4/161 (1977)

13) B.M.U.Scherzer, Ion solid interactions in fusion reactors, J.Vac.Sci.Technol. Vol.13, No 1, 420 (1976)

14) W VII A Team, Ohmic heating in the W VII A Stellarator IAEA-CN-35/D2 (1976)

Figure Captions:

Fig.1 Projection of the path of fast injected particles onto a meridional plane during thermalization. Collisions are marked by crosses. Three examples are given for each configuration.

Fig.2-4 Captured fraction of the neutral beam along the injection path (upper extremities). The product of the captured fraction and heating efficiency in the specified section is given by the lower extremities. The sladed area is thus proportional to the energy loss.

Fig.2 stellarator case

Fig.3 hybrid case

Fig.4 tokamak case

Fig.5 Captured fraction of the neutral beam along the injection path.

a) beam capture without impurities

b) beam capture with oxygen impurities (approx. 1%)

c) beam capture with oxygen impurities and Fe-impurities (approx. 0.1%) due to sputtering

Table I

	Configuration type	Heating efficiency W	Sputtered Fe flux / Beam intensity	Fe density ($\tau_p \approx 20$ ms)	Radiated power	Effective heating efficiency W′
$T_{e,max} = 0.3$ keV	a) "pure stellarator"	(40 ± 3.5) %	$(4.5 \pm 0.25)\ 10^{-3}$	$(2 \pm 0.1)\ 10^{11}$	290 kW	19.1 %
	b) "hybrid"	(67.5 ± 2) %	$(2.5 \pm 0.2)\ 10^{-3}$	$(1.1 \pm 0.1)\ 10^{11}$	156 kW	56.3 %
	c) "tokamak case"	(80 ± 2) %	$(1.35 \pm 0.2)\ 10^{-3}$	$(6 \pm 1.0)\ 10^{10}$	87 kW	74 %
$T_{e,max} = 1$ keV	a) "pure stellarator"	(13 ± 2) %	$(5.7 \pm 1)\ 10^{-3}$	$2.5 \cdot 10^{11}$	230 kW	radiated power is greater than injected power * W
	b) "hybrid case"	(37 ± 6) %	$(4.3 \pm 0.3)\ 10^{-3}$	$1.9 \cdot 10^{11}$	174 kW	25 %
	c) "tokamak case"	(47 ± 3) %	$(3.7 \pm 0.3)\ 10^{-3}$	$1.6 \cdot 10^{11}$	150 kW	36 %

STELLARATOR

HYBRID

TOKOMAK

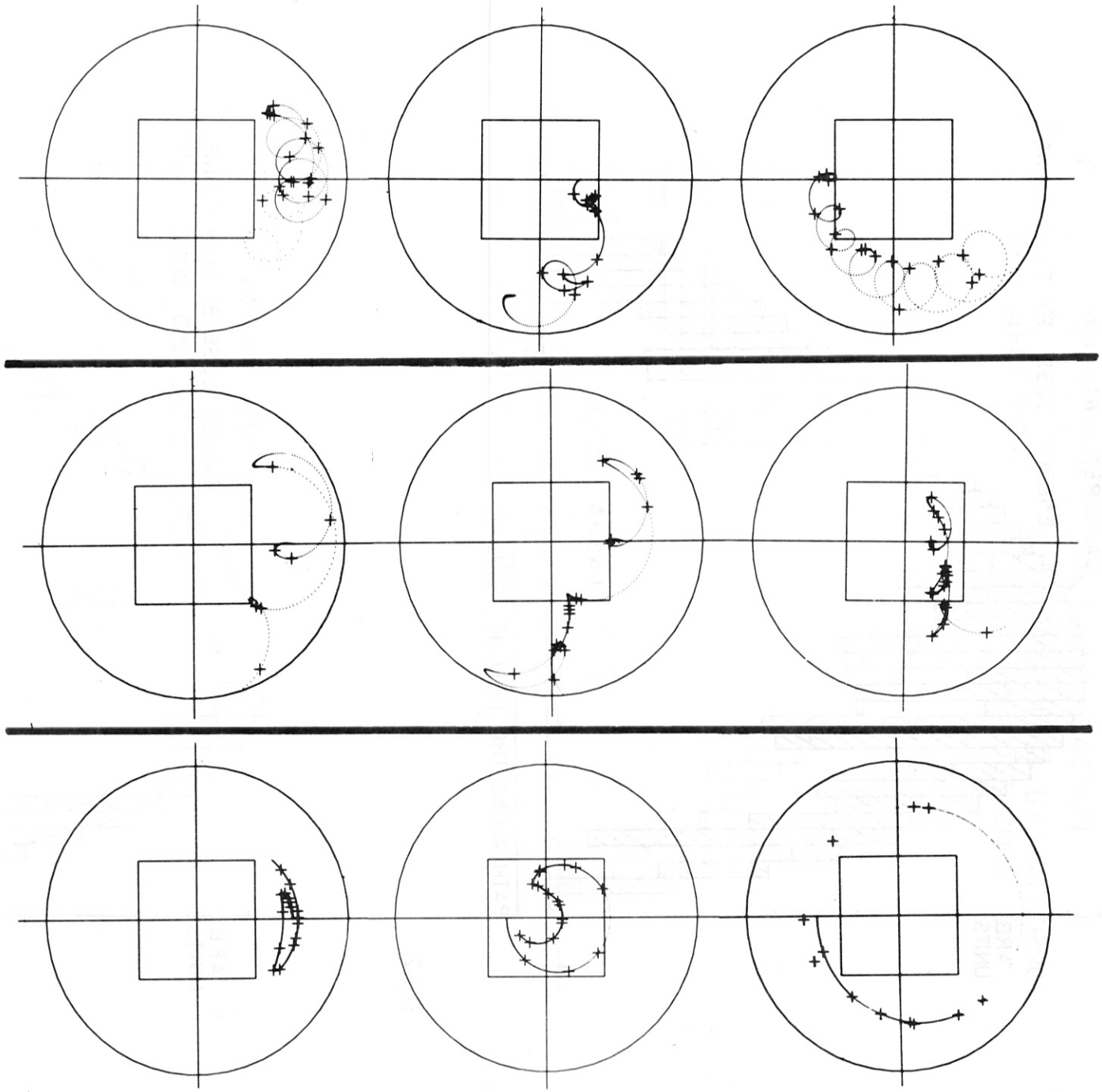

FIG. 1

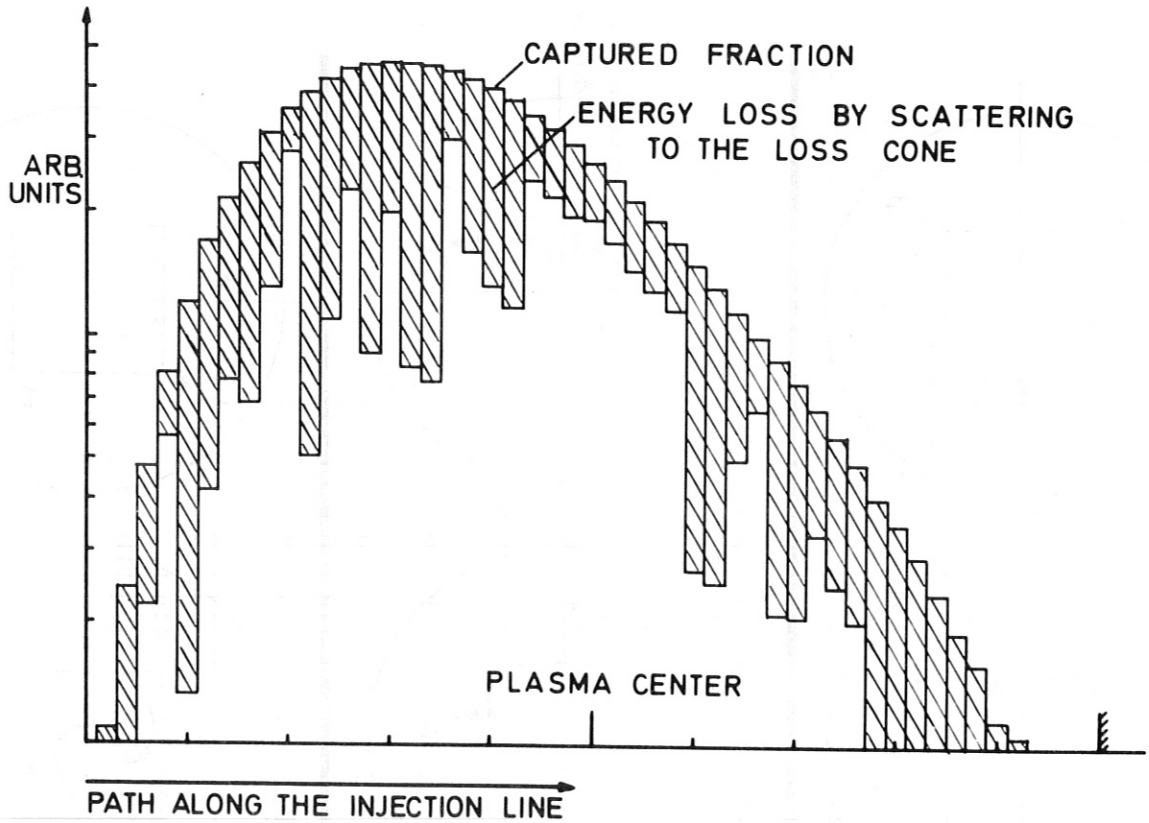
CAPTURED FRACTION
ENERGY LOSS BY SCATTERING
TO THE LOSS CONE
ARB.
UNITS
PLASMA CENTER
PATH ALONG THE INJECTION LINE

Fig.2

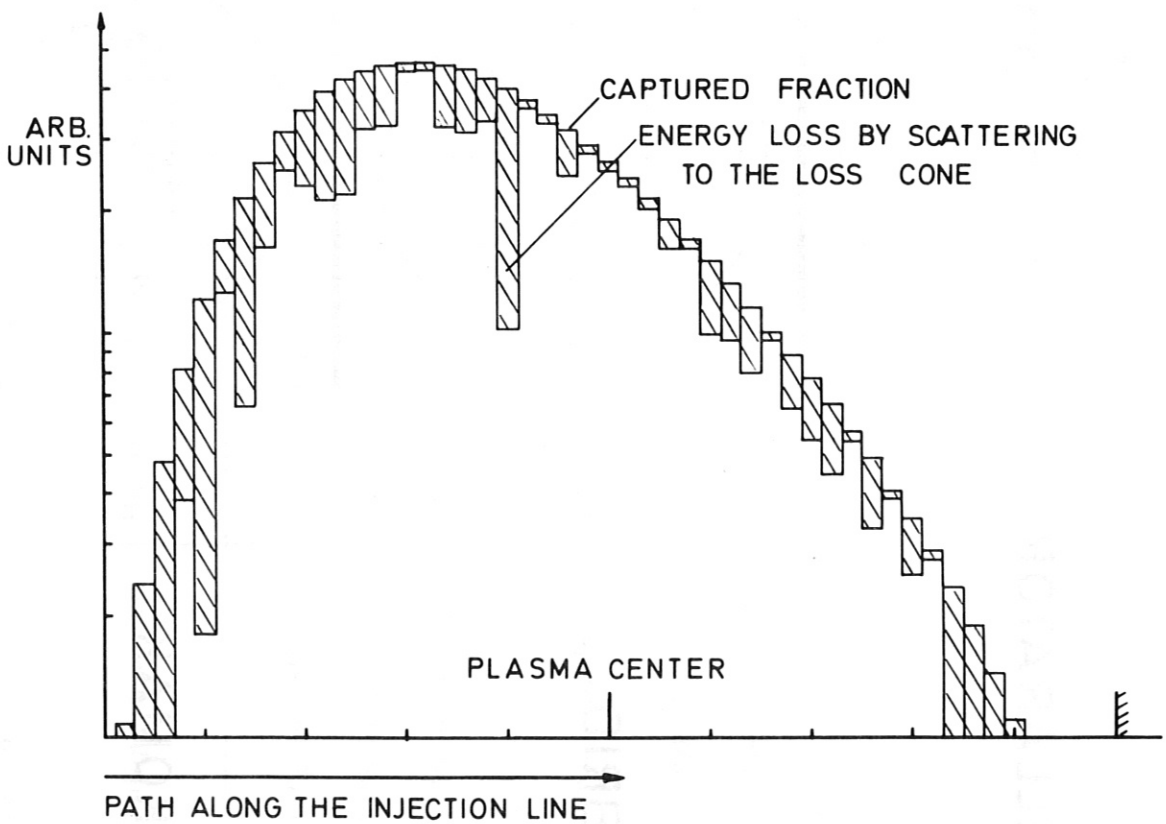
CAPTURED FRACTION
ENERGY LOSS BY SCATTERING
TO THE LOSS CONE
ARB.
UNITS
PLASMA CENTER
PATH ALONG THE INJECTION LINE

Fig.3

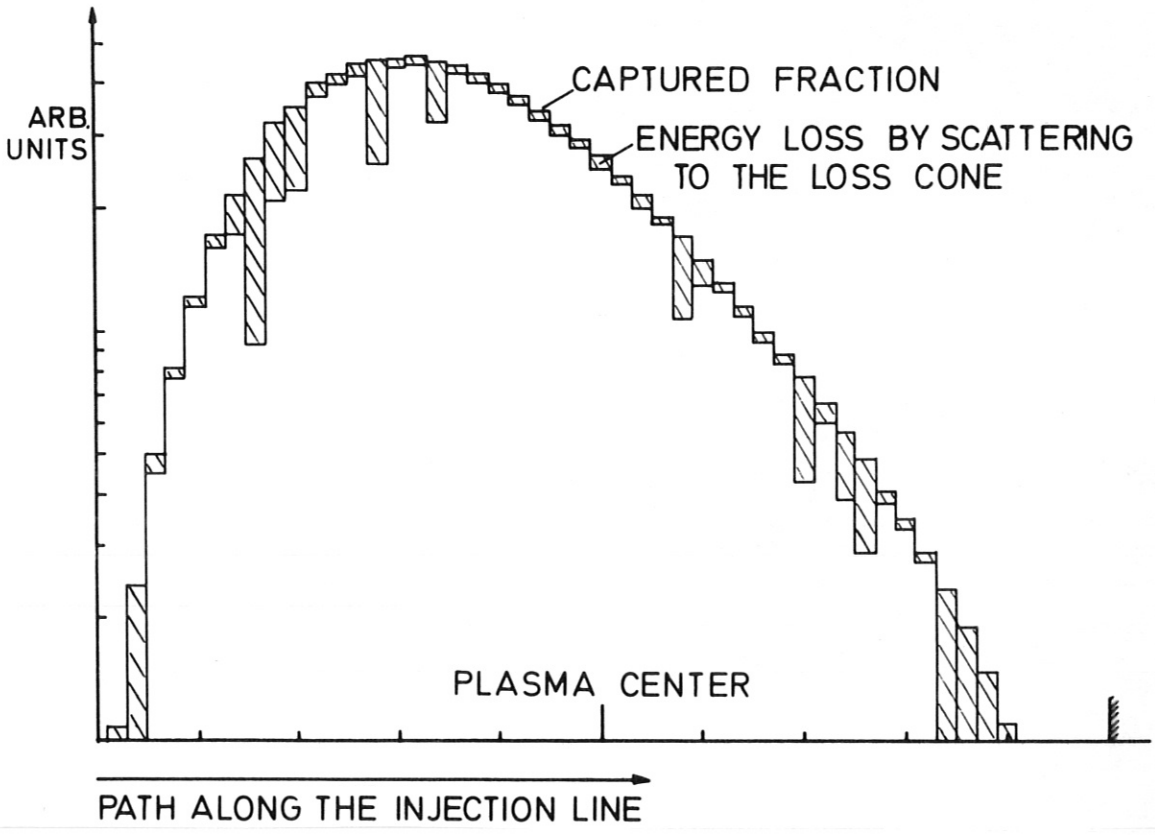
ARB.
UNITS
CAPTURED FRACTION
ENERGY LOSS BY SCATTERING
TO THE LOSS CONE
PLASMA CENTER
PATH ALONG THE INJECTION LINE

Fig.4

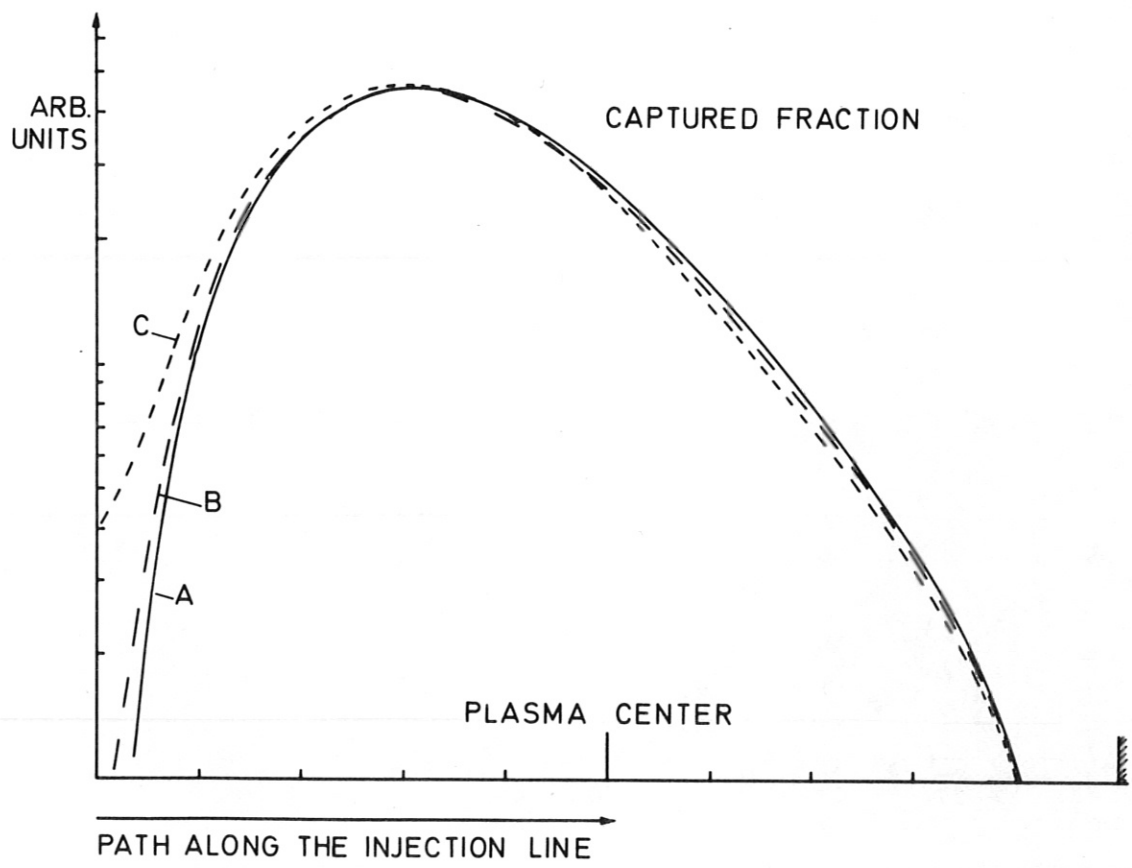
ARB.
UNITS
CAPTURED FRACTION
C
B
A
PLASMA CENTER
PATH ALONG THE INJECTION LINE

Fig.5